Answers to Anonymous Referee 2 on the paper 'Does the rotational direction of a wind turbine impact the wake in a stably stratified atmospheric boundary layer?'

Englberger et al.

Specific comments

1

Title: Although titles in the form of a question can generate curiosity, I find it more impactful to simply state the main hypothesis of the study, such as for example: Parametric study on the effects of wind veer and wind turbine rotation direction on the structure and recovery rate of the mean wake.

We think it is a matter of style. In this work, we think a question is suitable as it is answered with a clear yes in the Conclusion.

2

Introduction: There is a mixture of future and present tense used throughout. Please be consistent. Careful editing of the text is needed throughout the manuscript to ensure clarity of the presentation, particularly clear physical explanations and accurate word choice.

We reread the text taking care of future and present tense.

For example, in the first paragraph of the Introduction. "The diurnal cycle is driven by shortwave heating during day and radiative cooling at night." Both are radiative processes, shortwave solar heating for the land surface and longwave radiative cooling. This is followed by a statement about forces acting on velocity: "The interaction between the Coriolis force acting on the velocity components. . ."

We added longwave in front of radiative cooling at night.

3

Pg 2: the review of previous research could be more descriptive. For example what methods are employed in the various studies to investigate stability dependence on the ABL? Are there any important features that have been regarding the wake of wind turbines operating in stable and convective boundary layers compared to neutral?

We added the skewness as additional feature in the SBL: The stability-dependent wind and turbulence conditions determine the entrainment of energy and momentum into the wake region and the resulting wake structure, with fast eroding wakes in convective conditions and wakes persisting further downwind in stably stratified conditions which are additionally characterized by a

1

skewed wake (Abkar et al., 2016; Vollmer et al., 2017; Englberger and Dörnbrack, 2018). This stability dependence has been investigated in numerical simulations for the SBL (Aitken et al., 2014; Bhaganagar and Debnath, 2014, 2015; Dörenkämper et al., 2015), the CBL (Mirocha et al., 2014), both of them (Abkar and Porté-Agel, 2014; Vollmer et al., 2017), or the complete diurnal cycle (Abkar et al., 2016; Englberger and Dörnbrack, 2018).

4

Pg 2, Line 24: I believe Hui Hu's group at Iowa State published a number of papers on wind tunnel experiments to investigate the counter rotating, dual-rotor turbine, starting around 2014. It would be good to provide a comprehensive review for studies considering rotor rotation given the focus.

This paper was cited as Wei et al. 2014.

5

Fig. 1: note that rotor blades must be rotating to generate axial thrust, however this affect may be modeled using a drag disk, not including the effect of conservation of angular momentum. If I understand the text, this is the approach represented by subfigures 2c and 2d, but the language used is a bit confusing. In Fig. 1c and 1d, there is only an axial force acting on the wake, no tangential one. Whereas in 1a, b, e, f there is also a tangential force. We just mentioned this in the introduction to present the problem. In chapter 2.2 it is explained in detail by the component $\boldsymbol{\beta_v} \in \{ 0, -1, 1 \}$.

'$\mathbf{F}_{WT}$ corresponds to the turbine-induced force and the scalar prefactors $\boldsymbol{\beta_v} = (1, \beta_v, \beta_w)$ to the rotation of the rotor. The Coriolis force is represented by the angular velocity vector of the Earth's rotation.'

and further:

'... In these simulations, only the prefactors β_v and β_w in Eq. 1 differ. A clockwise wake rotation is defined by $\beta_v = -1$ and $\beta_w = 1$, a counterclockwise wake rotation by $\beta_v = 1$ and $\beta_w = -1$, and no rotation by $\beta_v = 0$ and $\beta_w = 0$, with $\beta_u = 1$ in each simulation. ...'

6

Section 2, Numerical Model Framework: The details of the model pertinent to the simulations conducted in this study should be explained in detail. It is appropriate to point to a former paper if validation is reported in support of this study. It is not clear if the paper cited provides these details. Nevertheless, the details of the specific model implementation in this study should be explained.

The details are given in Eq. 1-3. Here we changed the environmental state e.g. v_e to the boundary-layer state v_{BL} to make it clearer. All terms are defined below.

Further, we expanded the explanation of the wind-turbine parametrization in 2.2.

Pg. 4: Equation 2 appears incomplete. It may be easier to follow if first the description of Equations 1-3 are provided followed by explanation of the terms and definition of each variable.

We added the missing term. Now Eq. 2 says:

$$\frac{d\Theta'}{dt} = -\mathbf{v}\nabla\Theta_e + \mathcal{H}$$

An explanation of each term is given in the paper following Eg. 2.

Details about the implementation of the turbulence closure and turbine actuator model should be included. Are the implementations similar to Wu and Porte-Agel, or C. Archer?

– Turbulence closure:

Details about the implementation of turbulence closure can be found in Schmidt and Schumann, 1989 and Margolin et al. 1999 (cited in the paper)

– Actuator model:

We expanded the explanation of the actuator model to:

'The axial $\mathbf{F}_x$ and tangential $\mathbf{F}_\Theta$ (Eqs. 9 and 10) turbine-induced forces ($\mathbf{F}_{WT} = \mathbf{F}_x + \mathbf{F}_\Theta$) in Eq. 1 are parametrized with the BEM method as rotating actuator disc including a nacelle and excluding the tower.

$$
\begin{aligned}
\left.\left|F_x\right|\right|_{x_0,y,z} &= \frac{1}{2}\rho_0 \frac{Bc}{2\pi r_{x_0,y,z}}(c_L\cos\Phi + c_D\sin\Phi) \\
&\times A_{x_0,y,z}\frac{u^2_{x_\infty,y,z}(1-a)^2}{\sin^2\Phi}
\end{aligned}
\tag{1}
$$

$$
\begin{aligned}
\left.\left|F_\Theta\right|\right|_{x_0,y,z} &= \frac{1}{2}\rho_0 \frac{Bc}{2\pi r_{x_0,y,z}}(c_L\sin\Phi - c_D\cos\Phi) \\
&\times A_{x_0,y,z}\frac{u_{x_\infty,y,z}(1-a)\Omega r_{x_0,y,z}(1+a')}{\sin\Phi\cos\Phi}.
\end{aligned}
\tag{2}
$$

Here, the centre of the rotor in x-direction is defined by the grid-point coordinate x_0. B represents the number of blades, c is the chord length of the blade, c_L is the lift coefficient, c_D is the drag coefficient, Φ is the angle between the plane of rotation and the relative streamwise velocity, and a' is the tangential induction factor. Following Hansen (2008), we calculate a and a' by an iterative procedure from the airfoil data. For the airfoil data, the 10 MW reference wind turbine from DTU (Bak et al., 2013) is applied, whereas the radius of the rotor as well as the chord length of the blades are scaled to a rotor with a diameter of 100 m. The upstream velocity $u_{x_\infty,y,z}$ is taken at the first upstream grid point in the x-direction and the corresponding y and z coordinates. With the exception of ρ_0 and B, all other parameters appearing in Eqs. 1 and 2 depend on the radius $r_{x_0,y,z}$ and vary spatially. Further, the rotation frequency Ω is set to 7 rpm. A more detailed description of the wind-turbine parametrization and the applied smearing of the forces, as well as all values used in the wind-turbine parametrization can be found in Englberger and Dörnbrack (2017, parametrization B).'

- Comparison:

  Porte-Agel: LES model and actuator disc model

  C. Archer: Wind Turbine and Turbulence Simulator and actuator line model

  Our paper: LES model EULAG and actuator disc model → Comparable to Porte-Agel, however, different numerical model and different wind turbine represented in the simulations. Not directly comparable to C. Archer. A comparison of our model with others can be found in Englberger and Dörnbrack (2017), as cited in the paper.

8

Please explain how the inflow velocity profile is imposed in the simulations. How is a proper turbulence profile established for each case?

We expanded the explanation in the paper with: 'The parametrization considers three 3 D wind fields (u, v, and w), resulting from a neutral ABL precursor simulation, which are modified by a stratification-dependent weighting, resulting from the SBL state of a diurnal cycle precursor simulation.'

We added a detailed description of the Reynolds stress tensor terms, especially regarding the differences resulting between the veered and the non-veered simulations and included an additional Figure as: 'The ABL flow (Eqs. 4-8) in combination with the impressed turbulence of a stably stratified regime result in exactly the same Reynolds stress tensor terms of $u'u'$, $w'w$, and $u'w'$ in V and NV whereas there are differences in $v'v'$, $'u'v'$, and $v'w'$ (Fig. 2(b)). In the height of the rotor, $u'v'$ is symmetric with respect to hub height and both $u'v'$ and $v'v'$ increase approaching the blade tip, whereas $v'w$ is marginal.'
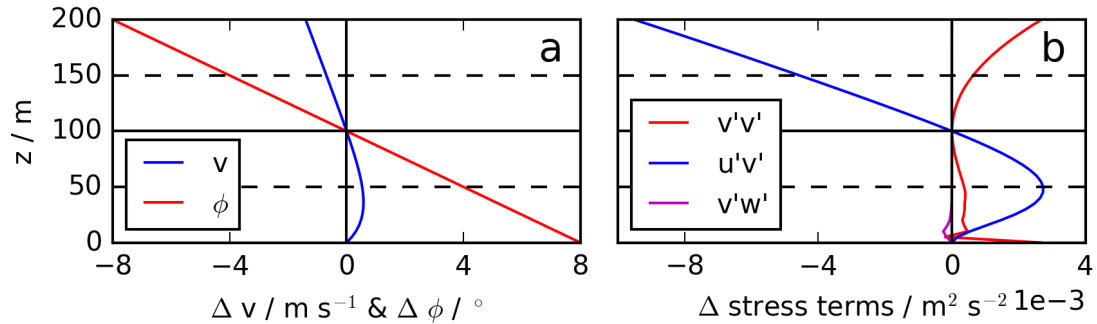

Figure 1. Differences in the initial conditions between V and NV for the spanwise velocity v and the incoming wind direction ϕ, whereas the differences are related to 270°, in (a) and the Reynolds stress tensor terms $v'v'$, $u'v'$ and $v'w'$ in (b).

9

Was the TKE model tested or calibrated to ensure the correct balance and transport is modeled in the wake region under the different flow and turbine operating conditions?

We use a standard TKE closure for LES. This means it is not calibrated for a specific problem. The coefficients result from Schmidt and Schumann (1989).

10

Pg. 5: How is the turbine model scaled? Based on geometry only? Or also considering operational characteristics? What are the details?

It is scaled based on the geometry. To our opinion this is valid considering the application of an acutator disc model with a grid spacing of 5 m. Further, the results of this study only depend on the rotational direction and are independent of the proposed wind turbine detailed blade characteristics, the only impact factor is the rotor diameter and the hub height interacting with the incoming wind profile.

11

Pg. 5: Please include a schematic and complete description of the simulation set-up, including size of the domain. What is the fraction of the channel cross-section occupied by the rotor disk? Is the grid spacing uniform? How many grid points represent the rotor? Are the turbine forces applied uniformly or based on some scheme related to the blade geometry and aerodynamics?

We included missing information.

- Size of domain is given with 512 x 64 x 64 grid points and a resolution of 5 m.

- The fraction of the channel cross-section is 100 m/(64*5 m) = 0.31 (See rotor diameter and domain size in 2.2).

- Yes, the grid spacing is uniform (see in the paper: with a horizontal and a vertical resolution of 5 m). We added uniform to the text.

- We applied the blade element momentum method (BEM) for the parametrization of the axial and tangential forces. The forces in the BEM have a radial dependency and further depend on the inflow velocity profile. Therefore, they are not uniform and depend on blade geometry and wind conditions. We expanded the description of the actuator parametrization in the text to make it clearer. (See 7)

12

Pg. 6: What is the corresponding land surface roughness, thermal stability, and latitudinal location represented by the imposed profiles uses in the simulations.

We apply a drag coefficient of 0.1 in our simulations. It represents homogeneous terrain and should be comparable to a surface

roughness of the order of O(0.01m).

Thermal stability: We missed it in the paper and included it as: 'The potential temperature is

$$\Theta_{BL}(z) = \frac{3\,K}{200\,m} z \tag{3}$$

in the lowest 200 m and 303 K above.'

Latitudinal location: We listed the Coriolis parameter $f = 1.0 \times 10^{-4}$ s^{-1}. With $f = 2\Omega sin(\phi)$, a latitude on earth of $\phi \approx 43°$ arises.

13

Regarding the turbine operation, what tip speed ratio and thrust coefficient are modeled? Are these typical operating conditions?

We included the information of 7 r.p.m. in the paper. This results with the upstream profile of Eq. 4 in a tip speed ratio of 0.58. As we apply the BEM approach, we do not have a single c_T value as in momentum theory. Therefore, we apply the values of the 10 MW reference wind turbine from DTU and cited them as Bak et al. (2013) in the paper.

14

Please check throughout and change "turbulent intensity" to "turbulence intensity".

We changed it.

15

Table 2: It is not clear from the later discussion of the results if both the 60 deg and 90 deg sectors are used in the analysis?

Only the results of 60° sectors are used. This is clarified in 2.3 in the paper: 'As the features are more distinctive for 60 ° and 25 m $\leq$ r $\leq$ 50 m sectors, these values are applied for the derivation of the sector characteristics in the following.'

16

Pg. 7: The use of index notation for velocity commonly refers to components of the vector, which may be confused with the (x, y, z) coordinates intended here.

'The indices of the grid points are denoted by $i = 1 \ldots n$, $j = 1 \ldots m$ and $k = 1 \ldots l$ in the x, y and z directions, respectively.' The use of discretized values in this way is standard for numerical purposes. This should not be linked to the Einstein notation.

17

Fig. 3: Labels on the contours are difficult to read due to crowding and may be improved for clarity.

We improved it.

18

Consider plotting distributions of turbulence intensity in the wake and provide any insight on the patterns seen for the distributions of the mean wake velocity.

We added vertical and spanwise profiles presenting the difference in velocity deficit ΔVD and ΔI between each two of the discussed simulations in the paper (See both Figures attached).

19

Section 3: Check the use of z, z_h, k_h, and k_*. There appears to be some inconstancy that may lead to confusion.

Here, z_h corresponds to the hub height of 100 m and k_h to the grid point index at hub height whereas k_* to the grid point index either on $z = 75$ m or 125 m. We have a typo in the caption of Fig. 4 (old manuscript version) (now Fig. 5), it should be $z = 125$ m not z_h. We changed it.

20

Pg 9, Lines 3-5: Would be useful to show plots of TKE to support the point about enhanced production effects on wake recovery.

See Nr. 18.

21

Pg 9, Line 10: Check NV_VR, should be NV_NR.

We changed it.

22

Figs 4 and 5: Quantification of the y-direction momentum budget could be used to support the assertion that the inflow veer and direction of wake rotation either partially cancel out or enhance wake deflection in the upper and lower portions of the wake.

We agree and added it in the results chapter as: 'This results from a weakening of the wake deflection angle in case of a clockwise rotating wind turbine and an amplification in case of a counterclockwise rotating wind turbine.'

23

Are there any data to support the simulation results of the wake you observe in the y-z plane?

We added a comparison to measurements: '...is similar to those observed the simulations of Abkar et al. (2016) (Fig. 16), Vollmer et al. (2017) (Fig. 9), and Englberger and Dörnbrack (2018) (Fig. 6) as well as in measurements of Bodini et al. (2017) (Fig. 12) and Brugger et al. (2019) (Fig. 4).'
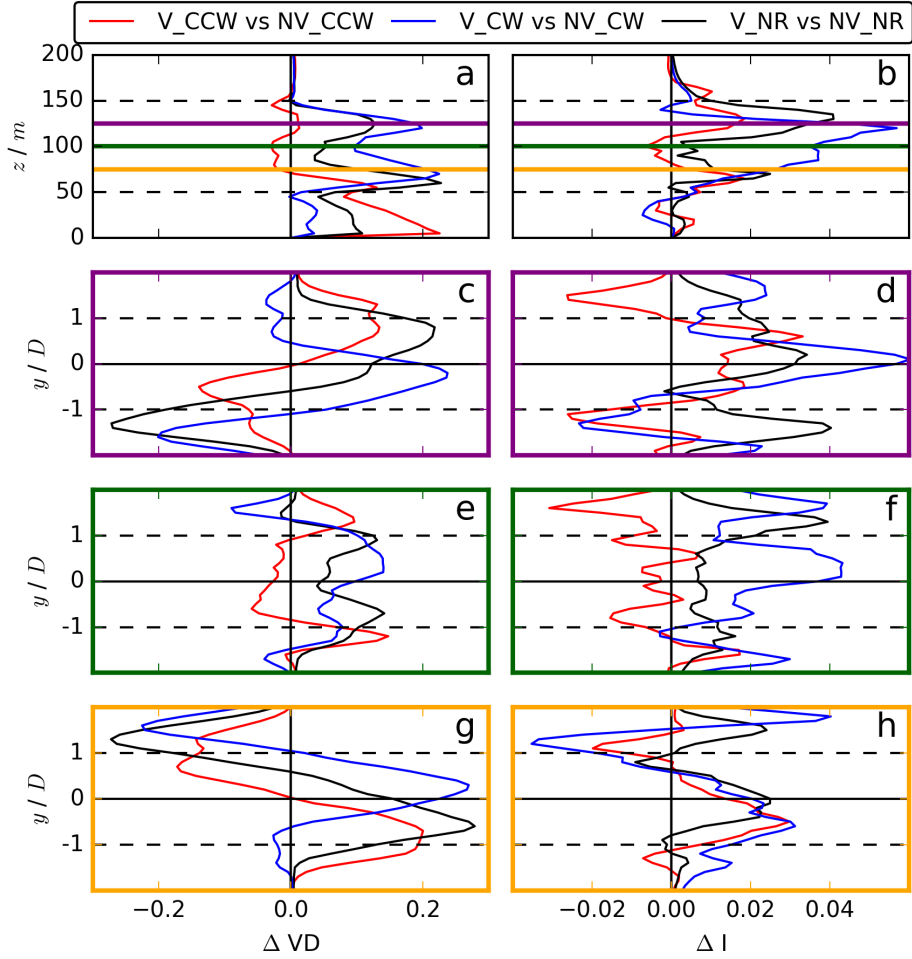
Figure 2. Vertical and spanwise profiles of ΔVD in (a), (c), (e), (g) and ΔI in (b), (d), (f), (h) at $10\,\mathrm{D}$. The spanwise profiles are plotted at 75 m (orange frame, (g), (h)), 100 m (hub height) (green frame, (e) (f)), and 125 m (purple frame (c), (d)). In panels (a) and (b), the coloured lines indicate the altitudes analysed in (c) - (h). Considering a comparison of two simulations A and B (see legend: A vs B), ΔVD is calculated as the difference between simulation B and simulation A $VD(B) - VD(A)$ and ΔI as the difference between simulation A and simulation B $I(A) - I(B)$. Therefore, $\Delta VD > 0$ and likewise $\Delta I > 0$ represent a more rapid wake recovery of simulation A in comparison to simulation B, related to a higher turbulence intensity level.
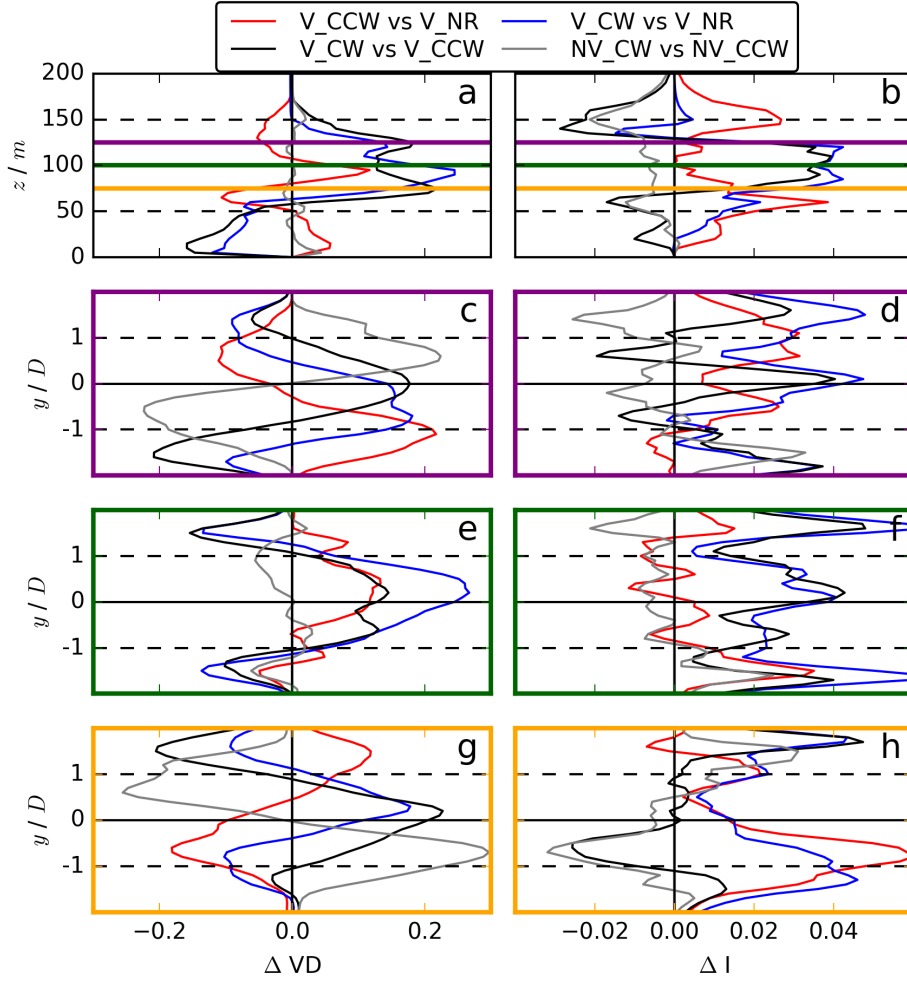
Figure 3. Vertical and spanwise profiles of ΔVD in (a), (c), (e), (g) and ΔI in (b), (d), (f), (h) at $10\,\mathrm{D}$. The spanwise profiles are plotted at 75 m (orange frame, (g), (h)), 100 m (hub height) (green frame, (e) (f)), and 125 m (purple frame (c), (d)). In panels (a) and (b), the coloured lines indicate the altitudes analysed in (c) - (h). Considering a comparison of two simulations A and B (see legend: A vs B), ΔVD is calculated as the difference between simulation B and simulation A $VD(B) - VD(A)$ and ΔI as the difference between simulation A and simulation B $I(A) - I(B)$. Therefore, $\Delta VD > 0$ and likewise $\Delta I > 0$ represent a more rapid wake recovery of simulation A in comparison to simulation B, related to a higher turbulence intensity level.

Fig. 7: Please explain the relatively stronger CW rotation in subfigure 7g compared to 7d and 7h. Why does the wake rotation switch from CCW sense to CW?

This is the fundamental heart of the paper. It is stated as short summary at the end of section 5: 'Consequently, the rotational direction of the flow in the near wake is determined by the rotational direction of the wind turbine, whereas the rotational direction of the flow in the far wake is determined by the ambient wind veer, often dictated by the direction of the Ekman spiral and thus by the sign of the Coriolis force and the hemisphere. If the rotational directions of the flow in the near wake and the boundary-layer flow intensify each other, the same rotational direction persists in the whole wake, as it is the case for a counterclockwise rotating wind turbine (V_CW). Otherwise, the rotational direction of the flow will change in the wake as for a clockwise rotating wind turbine under veered inflow conditions at night in the Northern Hemisphere (V_CCW).'

To make it more clear, we now added a short and informative explanation in the Conclusion: 'The LESs are controlled by the rotational direction of the wind-turbine wake imposed by the blades (clockwise (CW) vs. counterclockwise (CCW) vs. no rotation (NR)) and the inflow wind profiles (wind veer (V) vs. no wind veer (NV)). In detail, in case of a non-rotating actuator, the rotation of the flow in the wake is only determined by the SBL regime. If the rotational direction of the wake and the SBL are the same, also one rotational direction persists in the whole wake, as it would be the case for counterclockwise rotating blades in the Northern Hemisphere (V_CW). In case of the common clockwise rotating blades (V_CCW), the rotational direction in the near wake, imposed by the rotor, differs from the rotational direction in the far wake, induced by the veering wind in the stably stratified regime in the Northern Hemisphere.'

You might consider quantifying the Circulation within the rotor region to quantitatively compare the cases.

We have thought about it. The aim of the paper is to state the difference in the flow field of the wake by changing the rotational direction. It does not present a specific case/location. Therefore, to our opinion, a quantification of the circulation is not mandatory, however we agree with the reviewer, it is essential if specific cases are simulated and compared and we will take it into account for future work.

Fig. 8: Please comment on the relatively strong counter rotating structures observed between the rotor and the corners of the domain. Might these be weaker if the domain were enlarged?

The structures of rotation surrounding the disc are the same for all three cases in Fig. 8. The upper left and lower right corner rotate clockwise while the upper right and the lower left rotate counterclockwise. This persists (at least) up to 7D in all three cases. In case of a non-rotating rotor (NV_NR), the pattern is rather symmetric to the nacelle, whereas the asymmetry and intensification of the 12-3 o'clock and 6-9 o'clock sectors in NV_CCW and the 9-12 o'clock and 3-6 o'clock sectors in NV_CW result from the corresponding rotational direction of the two cases. Due to continuity equation, counter-rotating

vortices are expected. Further, the vorticity of these vortices is rater small in comparison to the main vortex induced by the actuator.

It could be a domain size effect, we cannot test it as the applied NBL precursor simulation used in the parametrization is limited to this spanwise domain. However, the effect only occurs in a SBL simulation with $v = 0$ NV, which is a rather artificial situation, whereas it is not the case in the important simulations with veering wind V. Further, due to the relatively small vorticity of this vortices it should not be really important for the results of NV and it is not important at all in the veering simulations V, representing the new insight of this study.

How might this affect the comparison with the simple model?

Considering the simple model, there is not effect expected. In the non-veered cases, the v and w graphs of Fig. 12 will overlap for the simulation as well as for the model results (plot not shown in paper).

27

Sect 4.1, Model Development: It would be useful to relate the models, particularly for the axial component of velocity to existing analytical wake models.

The intention of our simple model is not to be included as computationally fast method in other calculations etc. It was only designed to show that a simple interaction of two physical process is responsible for the completely different behaviour of v and w in the wake. u in the simple model is only of minor importance. Therefore, we do not consider the simple model as analytical wake model. At least not at this stage. However, for future work we will consider it.

For example, what is the physical meaning of the 0.3 used in Eqn. 9?

The physical meaning of the 0.3 factor is explained as: 'We apply a fraction of 0.3, which can be related to $VD_{max} = 0.7$ of the rotating disc simulations in Fig. 3.' It is basically connected the the deceleration of the velocity field behind the disc at about 70% due to the axial force resulting from the wind turbine parametrization, however, not to a deceleration of the streamwise velocity to 0.

It can also be related to the axial induction factor a, having the same definition as VD. To make to more clear, we added this explanation to make it more clear: 'We apply a fraction of 0.3, which can be related to $VD_{max} = 0.7$ of the rotating disc simulations in Fig. 3 and consequently to an axial induction factor a of 0.7, resulting in a fraction of $0.3 = (1-a)$, as it is the case by calculating the axial force with Momentum Theory Manwell et al. (2002); Hansen (2008).'

What are the axial and tangential induction factors used and are they appropriate for the turbine being modeled?

The model is composed of the ABL interacting with a Rankine Vortex, which is characterized by R and ω. No specific blade characteristics etc. are considered here. Therefore, no comparison of the simple model towards the BEM method is possible. The simple model does not include any turbine characteristics besides R and Ω.

28

Be sure to define all variables and subscripts used throughout the model development. For example, _RV, _M, _fad are not explicitly defined.

We added RV to Rankine Vortex: 'The wind-turbine model includes the axial turbine-induced force $\mathbf{F}_x$, as well as the tangential turbine-induced force $\mathbf{F}_\Theta$, which correspond to a Rankine Vortex (RV)'

We also added M to the simplified wake model: 'From a linear superposition results for the developed simplified wake model (M): '

_fad was described as: 'The downstream erosion of v_{WT} and w_{WT} with x_{fad} corresponding to a prescribed decay distance at which the atmospheric boundary-layer flow determines the rotational direction of the wake ...'

29

Eqns $18 - 20$, Given the premise that at least some of the flow conditions are caused by thermal stability, how could stability be included in the model, as the normal and shear components of turbulence fluxes will significantly affect the wake evolution.

This is an interesting topic, however, it would request basically a new model. As it does not contribute to the rotational direction of the wake, we do not consider it in this work.

30

How are the values of the parameters x_rec, x_fad, gamma, and delta chosen? Is it possible to estimate them without the flow data from simulations?

The values of x_{rec} and x_{fad} are obtained from the simulation results (see Fig. 12 left column). The magnitude of γ and δ result from archiving the best possible agreement between the model results and the simulation results. We added it as: 'The values of γ and δ are determined by empirical fitting.' We consider empirical fitting appropriate, as the values of δ and γ only modify the amount of v and w downwind, however, not the sign of both.

31

Pg 16, Line 14: Please check the single sentence paragraph.

We agree and combined it the the following paragraph describing the situation in detail.

32

Fig 9: It would be easier to compare the model with the LES output if they were plotted together and instead separate the CCW and CW cases. Note that the legend above the figure does not coincide with the figure description below for the vertical velocity plots.

We agree, this way of plotting would make it more easy to compare the difference between simulation and simplified model.

Our intent with this figure is to show the rotational direction impact in the simulations and especially in the model. We think this will be more transparent by plotting the simulation results and the simplified model results separately.

We changed the legend.

33

Please check that average velocity is defined and used consistently. Note in Fig 9, an overbar is used, but not in the figure description or elsewhere.

We changed in the legend u, v, and w to $\overline{u}$, $\overline{v}$, and $\overline{w}$.

Are the plotted data based on the 60 deg or 90 deg sectors defined in Table 2?

All data correspond to the 60° averages see 2.3: 'As the features are more distinctive for 60° and 25 m $\leq$ r $\leq$ 50 m sectors, these values are applied for the derivation of the sector characteristics in the following.' See comment 15.

34

Consider comparing the results to field data. In particular, there are a number of case experiments that have used lidar to measure the wake. Even if not the data are not directly compatible due to different turbine models or operating conditions, it would be useful to see if measurements see the same trends presented in this study.

We compared specific features (skewness) of the wake structure arising in the SBL in combination with wind veer to measurements: Bodini et al. (2017), Brugger et al. (2019). We can only compare the clockwise rotating blade simulations, therefore no comparison regarding the impact of the rotational direction is possible with field measurements.

35

Section 5: It is not clear if thermal stability was actually modeled, or only the Ekman spiral effect on the wind direction. The language used throughout the manuscript may contribute to confusion about what physics are considered in this study. This can be avoided by using explicitly clear language.

We added the definition of Θ, see 12. Further in Section 5, we added 'a lapse rate of 3 K / 200 m' in the text to make it more clear that our simulated stable boundary layer consists of a lapse rate which is combined with a veering wind representing the Ekman spiral.

36

Statements in the Conclusion that provide interpretation with various supporting references should be moved up to the Discussion. The Conclusion should focus on the main outcomes of the present study.

This is a matter of style. As the conclusion is relatively brief we think the comparison with other work is appropriate in this conclusion. Further, we refer to Schimel (2012) for writing the conclusion.

References

Abkar, M. and Porté-Agel, F.: The effect of atmospheric stability on wind-turbine wakes: A large-eddy simulation study, in: Journal of Physics: Conference Series, vol. 524, p. 012138, IOP Publishing, https://doi.org/10.1088/1742-6596/524/1/012138, 2014.

Abkar, M., Sharifi, A., and Porté-Agel, F.: Wake flow in a wind farm during a diurnal cycle, Journal of Turbulence, 17, 420–441, https://doi.org/10.1080/14685248.2015.1127379, 2016.

Aitken, M. L., Kosović, B., Mirocha, J. D., and Lundquist, J. K.: Large eddy simulation of wind turbine wake dynamics in the stable boundary layer using the Weather Research and Forecasting Model, J Renew Sust Energy, 6, 1529–1539, https://doi.org/10.1063/1.4885111, 2014.

Bak, C., Zahle, F., Bitsche, R., Kim, T., Yde, A., Henriksen, L. C., Hansen, M. H., Blasques, J. P. A. A., Gaunaa, M., and Natarajan, A.: The DTU 10-MW reference wind turbine, in: Danish Wind Power Research 2013, 2013.

Bhaganagar, K. and Debnath, M.: Implications of Stably Stratified Atmospheric Boundary Layer Turbulence on the Near-Wake Structure of Wind Turbines, Energies, 7, 5740–5763, https://doi.org/10.3390/en7095740, 2014.

Bhaganagar, K. and Debnath, M.: The effects of mean atmospheric forcings of the stable atmospheric boundary layer on wind turbine wake, Journal of Renewable and Sustainable Energy, 7, 013 124, https://doi.org/10.1063/1.4907687, 2015.

Bodini, N., Zardi, D., and Lundquist, J. K.: Three-dimensional structure of wind turbine wakes as measured by scanning lidar, Atmospheric Measurement Techniques, 10, 2017.

Brugger, P., Fuertes, F. C., Vahidzadeh, M., Markfort, C. D., and Porté-Agel, F.: Characterization of Wind Turbine Wakes with Nacelle-Mounted Doppler LiDARs and Model Validation in the Presence of Wind Veer, Remote Sensing, 11, 2247, 2019.

Dörenkämper, M., Witha, B., Steinfeld, G., Heinemann, D., and Kühn, M.: The impact of stable atmospheric boundary layers on wind-turbine wakes within offshore wind farms, Journal of Wind Engineering and Industrial Aerodynamics, 144, 146–153, https://doi.org/10.1016/j.jweia.2014.12.011, 2015.

Englberger, A. and Dörnbrack, A.: Impact of Neutral Boundary-Layer Turbulence on Wind-Turbine Wakes: A Numerical Modelling Study, Boundary-Layer Meteorology, 162, 427–449, https://doi.org/10.1007/s10546-016-0208-z, 2017.

Englberger, A. and Dörnbrack, A.: Impact of the diurnal cycle of the atmospheric boundary layer on wind-turbine wakes: a numerical modelling study, Boundary-layer meteorology, 166, 423–448, https://doi.org/10.1007/s10546-017-0309-3, 2018.

Hansen, M. O.: Aerodynamics of wind turbines, vol. 2, Earthscan, London and Sterling, UK and USA, 181 pp, 2008.

Manwell, J., McGowan, J., and Roger, A.: Wind Energy Explained: Theory, Design and Application, Wiley: New York, NY, USA, 134 pp, 2002.

Mirocha, J. D., Kosović, B., Aitken, M. L., and Lundquist, J. K.: Implementation of a generalized actuator disk wind turbine model into the weather research and forecasting model for large-eddy simulation applications, J Renew Sust Energy, 6, 013 104, https://doi.org/10.1063/1.4861061, 2014.

Schimel, J.: Writing science: how to write papers that get cited and proposals that get funded, OUP USA, 2012.

Schmidt, H. and Schumann, U.: Coherent structure of the convective boundary layer derived from large-eddy simulations, J Fluid Mech, 200, 511–562, https://doi.org/10.1017/S0022112089000753, 1989.

Vollmer, L., Lee, J. C., Steinfeld, G., and Lundquist, J.: A wind turbine wake in changing atmospheric conditions: LES and lidar measurements, in: Journal of Physics: Conference Series, vol. 854, p. 012050, IOP Publishing, https://doi.org/10.1088/1742-6596/75/1/012003, 2017.